ACS OMEGA

http://pubs.acs.org/journal/acsodf

Article

Can We Predict Interface Dipoles Based on Molecular Properties?

Johannes J. Cartus, Andreas Jeindl, and Oliver T. Hofmann*

Cite This: *ACS Omega* 2021, 6, 32270−32276

Read Online

ACCESS | Metrics & More | Article Recommendations | Supporting Information

ABSTRACT: We apply high-throughput density functional theory calculations and symbolic regression to hybrid inorganic/organic interfaces with the intent to extract physically meaningful correlations between the adsorption-induced work function modifications and the properties of the constituents. We separately investigate two cases: (1) hypothetical, free-standing self-assembled monolayers with a large intrinsic dipole moment and (2) metal−organic interfaces with a large charge-transfer-induced dipole. For the former, we find, without notable prior assumptions, the Topping model, as expected from the literature. For the latter, highly accurate correlations are found, which are, however, clearly unphysical.

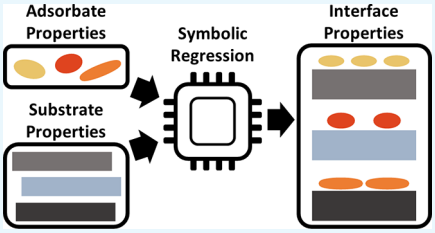

INTRODUCTION

The level alignment of metal−organic interfaces has been subject to much attention from both fundamental[1−4] and engineering research, especially in the context of organic electronics.[5−8] Suboptimal choices in the design of interface materials can lead to poor device performance, for example, because of electrical resistances caused by large charge-injection barriers.[5] However, these injection barriers, which depend on the offset between the metal's Fermi energy and the molecular levels,[2] can be optimized by adsorbing a so-called charge-injection layer onto the metal. These layers change the level alignment because of the emergence of an adsorption-induced potential jump[1−4] (often termed "interface dipole"), $\Delta\Phi$.

Currently, $\Delta\Phi$ must be determined separately for every substrate/adsorbate combination, either experimentally or via first-principles calculations, but both options are expensive and laborious.[9] A prediction, or at least a solid estimate, of $\Delta\Phi$ based solely on the properties of the isolated adsorbate and substrate would significantly speed up the optimization process for inorganic/organic interfaces. However, although there are several (often conflicting) models that relate molecular properties to $\Delta\Phi$ (such as the induced density of interface states model,[10−13] the integer charge-transfer model,[14−16] or pinning on the lowest unoccupied molecular orbital (LUMO)[17−21]), an explicit expression describing the interface dipole via the properties of the constituents is yet to be put forth. In fact, it is not yet clear whether such an expression can be formulated based solely on the properties of the interface constituents at all.

In this work, we attempt to extract an analytic expression by a combination of high-throughput first-principles calculations and symbolic regression. In its most simple formulation, symbolic regression takes a number of input properties (e.g., the molecular dipole moment, the ionization energy, etc.; see below) and combines them via mathematical operators (e.g., multiplication, exponentiation, etc.) into more complex equations (i.e., analytic models). These expressions are then fitted against a target quantity (e.g., $\Delta\Phi$). Ideally, the best-fitting models correspond to the "natural laws" that govern the physics underlying the data.[22,23] This approach can be seen as a one-dimensional variant of the sure independence screening sparsifying operator (SISSO) method[24] (see the Supporting Information). However, the complexity from additional SISSO dimensions is not necessarily required (or helpful) for detecting physical relationships (see the Supporting Information).

When studying the interface-dipole-induced work function change, it has become customary to dissect it into two components:[18,25] the contribution that arises from the bonding to the substrate, $\Delta\Phi^{\mathrm{Bond}}$, and the jump of the electrostatic potential that would be induced by the adsorbate alone, $\Delta\Phi^{\mathrm{Mol}}$:

$$\Delta\Phi = \Delta\Phi^{\mathrm{Mol}} + \Delta\Phi^{\mathrm{Bond}} \quad (1)$$

Because it is difficult, if not impossible, for symbolic regression to identify two different effects of similar magnitude (for explanation see the Supporting Information), here, we aim at obtaining analytical models for $\Delta\Phi^{\mathrm{Mol}}$ and $\Delta\Phi^{\mathrm{Bond}}$ separately.

RESULTS AND DISCUSSION

Adsorbate Dipole. Starting with the adsorbate-dipole-induced potential jump $\Delta\Phi^{\mathrm{Mol}}$, we design several planar heteroaromatics with substantial in-plane dipole moments

Received: September 14, 2021
Accepted: November 2, 2021
Published: November 14, 2021

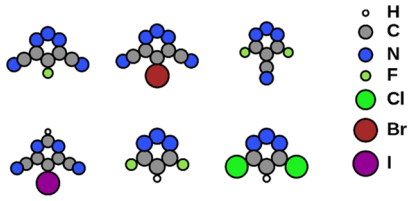

Figure 1. The six heteroaromatic molecules we used to build free-standing self-assembled monolayers.

through specific substitution of halogens and nitrogen. From these, we select the six molecules with the largest electron affinity (shown in Figure 1), which will be useful for the investigation of $\Delta\Phi^{\mathrm{Bond}}$ later in this work. We then create hypothetical, free-standing self-assembled monolayers (i.e., without substrates) by placing the molecules, with their intrinsic dipole moments aligned in the z-direction, in various unit cells with various side lengths (12.5−30 Å) and angles (45, 60, 75, and 90°). The combination of molecules and unit cells yields 360 different systems. An example is depicted in the Supporting Information. For these systems, we obtain $\Delta\Phi^{\mathrm{Mol}}$ by performing dispersion-corrected density functional theory (DFT) calculations with the Fritz Haber Institute ab initio materials simulations package (FHI-aims)[26] using the Perdew−Burke−Ernzerhof (PBE) exchange-correction functional[27] and a dipole correction[28] (further details are given in the Methods section).

To extract analytic models for $\Delta\Phi^{\mathrm{Mol}}$, our symbolic regression algorithm takes various properties of the interface or the isolated molecules in the gas phase as input. We then combine these input properties via mathematical operations to build analytical expressions. To keep the number of possible expressions tractable, we adhere to the following protocol: in the first step, we exhaustively create products of up to three input parameters and their reciprocals, that is, we create expressions of the form $F(x, y, z) = x^a y^b z^c$ with three different input parameters x, y, z and exponents a, b, $c \in \{-1,0,1\}$. In the second step, we create additional expressions by applying the nonlinear mapping $F'(F_i, F_j) = F_i/(F_j + 1)$ to all possible pairs of expressions, with the restriction that the factors x, y, z in F_i and F_j can only differ in a single input parameter. Finally, all created expressions are evaluated using the input parameter values from the systems in the data set. For each analytical expression, a linear fit against $\Delta\Phi^{\mathrm{Mol}}$ is performed, and the best-performing fit (in terms of its root-mean-square-error, RMSE) is reported.

Because the resulting set of analytical expressions grows very fast with the number of input parameters, a thoughtful selection is required. Here, we use the following properties for the isolated molecules in the gas phase as input parameters: the orbital energy of the highest occupied molecular orbital ($\varepsilon_{\mathrm{HOMO}}$) and of the LUMO ($\varepsilon_{\mathrm{LUMO}}$), the ionization potential (IP) and the electron affinity (EA) via the ΔSCF approach (see the Methods section), the molecular dipole moment μ, and the molecular polarizability α along the direction of the dipole moment. In addition, we provide the lengths of the unit cell vectors (a,b), the minimum distance between two atoms (d_{min}), and C_Σ, the infinite sum of cubed reciprocal distances from a dipole to all its neighbors, as geometry-dependent input parameters. The latter often appears in the electrostatic description of collective electric fields of dipoles.[29] A compilation of all used parameters is provided in Table 1.

Table 1. Compilation of Input Parameters Used to Construct the Candidate Analytical Expressions for $\Delta\Phi^{\mathrm{Mol}}$

name	description
a,b	unit cell side lengths
d_{min}	minimum distance between atoms of periodic replicas of adsorbate molecules
ρ	dipole density (number of molecules per area)
C_Σ	infinite sum of cubed reciprocal distances r_i from a molecule to all its neighbors: $C_\Sigma = \sum_i r_i^{-3}$.
$\varepsilon_{\mathrm{HOMO}}$, $\varepsilon_{\mathrm{LUMO}}$	orbital energies of the isolated molecule
IP, EA	vertical IP and EA of the isolated molecule
μ_z	z-component of the single molecule dipole moment in vacuum
α_{zz}	molecular polarizability along the direction of the dipole moment

For our systems, the expression with the lowest RMSE (3.3 meV) we found is shown in eq 2.

$$\Delta\Phi^{\mathrm{Mol}} \propto \frac{\mu_z \rho}{\alpha_{zz} C_\Sigma + 1} \tag{2}$$

The excellent agreement between the prediction of $\Delta\Phi^{\mathrm{Mol}}$ via eq 2 and the "true" values originally obtained by DFT is displayed in Figure 2a. Eq 2 is exactly the Topping model, which is expected from classical electrostatics[29−31] and was previously suggested by numerous other theoretical[32−34] and experimental[31,35] studies.

While finding the Topping model from our data shows the validity of our approach, it is important to emphasize that this success is by no means guaranteed. Obviously, we could only find eq 2 because we allowed for the nonlinear mathematical operation and because we provided C_Σ as input parameter. Neither of these would necessarily be intuitive, but without either of these, we would only obtain physically incorrect solutions. Interestingly, when including additional systems that are too densely packed (i.e., when the point-dipole approximation underlying the Topping model[29] starts to break down), some of these unphysical models exhibit even lower RMSE values (i.e., perform even better) than the physically correct expression. Nevertheless, under the correct boundary conditions, the "correct" physical picture can be accurately obtained from our data.

Bond Dipole. As the second step, we turn to $\Delta\Phi^{\mathrm{Bond}}$. This term contains all effects of $\Delta\Phi$ arising from the interaction of the adsorbate with the substrate, such as charge transfer, Pauli pushback, formation of covalent bonds, and so forth.[1−4] In this work, we focus on charge transfer only because it is (a) relatively straightforward to separate from the other effects and because (b) one would expect that the molecular properties that govern can be easily tuned via chemical modifications of the adsorbate.

To increase the diversity in our data set (compared to the previous section), here, we use a total of 28 different heteroaromatic molecules, consisting of the 6 molecules used before and 22 additional molecules that are based on naphthalene as a backbone to allow for more varied molecular properties (for details, see the Supporting Information). A challenge when considering $\Delta\Phi^{\mathrm{Bond}}$ is that it is known to depend strongly on the geometry the adsorbate assumes. For instance, whether a molecule adsorbs flat-lying or upright-standing can change $\Delta\Phi^{\mathrm{Bond}}$ by more than 1 eV[36−38] because of the associated change in the molecule's ionization energies.[39] Similarly, $\Delta\Phi^{\mathrm{Bond}}$ is strongly affected by the

https://doi.org/10.1021/acsomega.1c05092
ACS Omega 2021, 6, 32270−32276

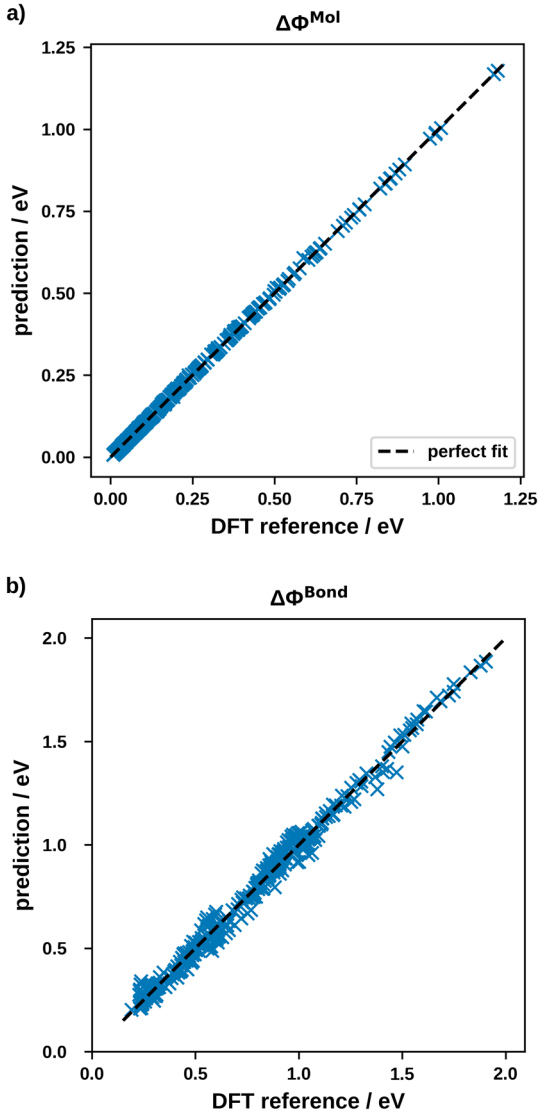

Figure 2. Prediction of (a) $\Delta\Phi^{\mathrm{Mol}}$ and (b) $\Delta\Phi^{\mathrm{Bond}}$ versus the DFT-calculated reference data. The dashed line marks a hypothetical perfect fit.

molecular coverage.[33,40,41] However, on metal substrates, most molecules adsorb in an approximately flat-lying geometry,[42] often slightly bent[17,43,44] or with a small tilt.[44−47] To simplify the physics to be described, here, we assume hypothetical geometries in which all molecules remain perfectly flat. This has the further advantage that their molecular dipole moment is parallel to the xy-plane, such that it does not contribute to $\Delta\Phi$. To remove any coverage-dependent effects, we use the same supercell, that is, adsorbate density, throughout. This geometry is an Ag(111) surface slab with five layers and a surface area of 5 × 5 Ag atoms. The large supercell ensures that there is only very little interaction between adjacent molecules. To focus on charge-transfer alone, we use hypothetical interfaces where the adsorption height is sufficiently large to inhibit wave-function overlap between the substrate and the adsorbate, thereby switching off any contributions from Pauli pushback or covalent bonds. In practice, we adsorb molecules at distances between 7 and 100 Å above metal slabs made of Ag, Al, In, Mg, and Na. In total, this results in 323 different interface systems to evaluate our expressions on.

Also, here, we must select suitable input parameters for the symbolic regression approach. We start by taking the ones suggested by the various models in the literature:

- The induced density of interface states implies a relation to the density of states at the Fermi level (a substrate property),[10,11] which we also include here.
- The so-called integer charge-transfer model postulates that charge transfer occurs via polaronic levels.[14−16] While polarons are a crystal quantity and their relation to purely molecular properties is not straightforward, here, we incorporate them approximately as the molecule's vertical EA and the relaxation energy E_{relax}. The latter refers to the difference between the energy of the singly charged molecule in the geometry of the neutral molecule and when it is fully optimized, that is, its internal reorganization energy. Because we are interested in work function changes, we use EA relative to the substrates' work function.
- Many previous theoretical calculations imply that $\Delta\Phi^{\mathrm{Bond}}$ is determined by the difference between the frontier orbital energies and the Fermi energy.[18,19]

We also add the polarizability of the molecule perpendicular to the aromatic plane, α_{zz}, and the HOMO−LUMO gap because it is a common measure for the reactivity of a molecule.[48] Furthermore, it is conceivable that image-charge effects play a role. As geometric properties, we therefore include the height of the molecule above the substrate's image plane position (for details, see the Supporting Information) and above the topmost layer as input parameters. A comprehensive compilation of input parameters is given in Table 2. Otherwise, we construct expressions as we did for $\Delta\Phi^{\mathrm{Mol}}$, that is, we build products F of up to three input parameters (or their reciprocals) and create additional expressions via the nonlinear mapping $F' = F_i/(F_j + 1)$ using the same conditions as above.

For the bond dipole, we find the best-performing expression to be as follows:

$$\Delta\Phi^{\mathrm{Bond}} \propto (\varepsilon_{\mathrm{LUMO}} - E_{\mathrm{F}})\frac{h}{h - z_{\mathrm{im}}}\frac{1}{1 + \left(\frac{\mathrm{IP} - \Phi}{h}\right)} \quad (3)$$

Table 2. Compilation of Input Parameters Used to Construct the Candidate Analytical Expressions for $\Delta\Phi^{\mathrm{Bond}}$

name	description
$\varepsilon_{\mathrm{LUMO}} - E_{\mathrm{F}}$	difference of the LUMO of the adsorbate and the Fermi energy of the substrate.
$\varepsilon_{\mathrm{HOMO}} - E_{\mathrm{F}}$	difference of the HOMO of the adsorbate and the Fermi energy of the substrate.
EA − Φ	difference of the EA of the adsorbate and the work function of the substrate.
IP − Φ	difference of the IP of the adsorbate and the work function of the substrate.
E_{relax}	relaxation energy of the adsorbate (see the main text).
DOS(E_{F})	density of states of the pristine substrate at the Fermi energy.
$h - z_{\mathrm{im}}$	adsorption height of the molecule w.r.t the image plane position.
h	adsorption height of the molecule w.r.t the uppermost substrate layer.
$\varepsilon_{\mathrm{LUMO}} - \varepsilon_{\mathrm{HOMO}}$	HOMO−LUMO gap.
α_{zz}	zz-component of the polarizability tensor of the adsorbate.

https://doi.org/10.1021/acsomega.1c05092
ACS Omega 2021, 6, 32270−32276

With an RMSE of 38 meV, it performs reasonably well (see Figure 2b), even if the RMSE is one order of magnitude worse than the Topping model for the $\Delta\Phi^{Mol}$.

Inspection of eq 3 reveals that it is almost exclusively dominated by the term ($\varepsilon_{LUMO} - E_F$). The second term, $h/(h - z_{im})$, is always larger than but close to 1 (between 1.0 and 1.5), because $h \gg z_{im}$ for the majority of systems in our data set. Conversely, the third term is also always close to one, but smaller (between 0.5 and 1.0), because within the units used here, the numerical value for IP-Φ/h is small for all systems. In fact, it must be stressed that this third term cannot carry any significance beyond numerics, as the physical dimensions of the featured parameters do not match. We allow for such "numeric terms" to achieve a greater variety in the generated expressions. Because the second and third term also counteract each other (both get closer to 1 as h increases), the $\Delta\Phi^{Bond}$ values predicted using eq 3 scatter only very little around $\varepsilon_{LUMO} - E_F$. This may, in principle, indicate that our computations yield noisy results for $\Delta\Phi^{Bond}$. However, our self-consistent field (SCF) procedure converged $\Delta\Phi$ to 10^{-4} eV (see the Methods section), that is, much too tight to allow for noise of this magnitude. Furthermore, we note that ε_{LUMO} is an auxiliary quantity from DFT. There is some debate about when orbital energies correspond to observables (e.g., photoemission resonances).[49] However, they always do depend on the chosen exchange-correlation functional, that is, the chosen theoretical method. In an earlier work, we have shown that there is no direct proportionality between ($\varepsilon_{LUMO} - E_F$) and $\Delta\Phi^{Bond}$ when going, for example, from semilocal to hybrid functionals.[19] In other words, in salient contrast to the Topping model found in eq 2, eq 3 fails to extract the physics that governs the charge transfer at the interface (rather, it merely shows an excellent correlation).

There are multiple possible reasons for this. In principle, it would be conceivable that some of our data are faulty. However, we can readily extract other physical relationships (see the Supporting Information), which attest to the fidelity of our results. Another possible explanation would be that we do not include the correct input parameters and mathematical operations or that we do not allow for sufficiently complex expressions. However, also various other additional input parameters and more varied exponents and (nonlinear) functions fail to yield physically meaningful results (see the Supporting Information). While this is no proof that we just did not include the "right" ingredients (such a proof is fundamentally impossible), it seems unlikely that the correct relation is an expression that is even more complex than what we already found for eq 3. Finally, we must face the hypothesis that our data, being synthetic, computed data with an approximate theory, just do not reproduce the underlying physics with sufficient accuracy.

Indeed, the PBE functional is known to have certain issues when describing charge-transfer systems. For example, when dissociating H_2^+ (i.e., placing the two H-cores far away from each other), it yields the unphysical solution of two protons with half an electron each, instead of a neutral H and a positively charged H^+ atom. Also here, we find that the molecules, even far above the surface (and thus completely unhybridized with it), are fractionally charged. In principle, a physically more correct solution could be a mixture of charged and uncharged molecules, that is, integer charge transfer. This could only be obtained by employing large supercells in combination with specifically tuned hybrid functionals.[19] However, the optimal functional would have to be determined separately for each system,[50] which incurs computational costs that are presently intractable. At the same time, it is not clear whether this would even solve the issue: because $\Delta\Phi$ depends on the average amount of charge transferred per area, not its distribution, a computation with hybrid functionals may not yield more accurate values. A further related problem is the self-interaction error of PBE. This effect not only causes the well-known underestimation of the band gap but it also makes the energies of the orbitals (including the LUMO) dependent on their occupation. This shift of the orbital energy may be superimposed to the shift of the orbital energy induced by $\Delta\Phi^{Bond}$, making it impossible for symbolic regression to extract either effect.

CONCLUSIONS

In summary, we attempted to extract the physics that govern the formation of interface dipoles at inorganic-organic interfaces. To that aim, we computed large data sets using semilocal DFT and applied symbolic regression to obtain functional relationships between the properties of the molecules (and the substrate) and $\Delta\Phi$. The approach was successful for the contribution of the molecular dipole, yielding the well-known Topping model. Conversely, for the charge-transfer contribution, we obtained a clearly unphysical result that depends on a DFT quantity rather than a molecular property. We tentatively attribute the failure to extract a clear physical relationship to the shortcomings of the underlying method (PBE). Despite the generally outstanding performance of dispersion-corrected PBE calculations for interfaces,[51−54] this advises that caution should be taken when computing interfaces with a notable charge-transfer character.

Moreover, the difficulty to extract the relevant physics for charge transfer even with a very large data set and an extensive combination of molecular and substrate parameters shows that the design of inorganic−organic interfaces with a predefined level alignment is nontrivial and will continue to be so. Even when minimizing the impact of the adsorbate geometry (which is extremely difficult to predict in the first place), and when simplifying the problem by avoiding quantum mechanical interactions (such as Pauli pushback and covalent bonds) as much as possible, we can only extract empirical correlations so far. For a comprehensive understanding and description of all effects at the interface, evidently much larger, more sophisticated data sets are still needed.

METHODS

All DFT calculations mentioned in the study were performed using FHI aims.[26] This code allows employing both open and periodic boundary conditions, that is, individual molecules and interfaces can be treated on the same footing. For all systems, we used tight basis sets and numerical defaults as shipped with release 201103. The PBE[27] exchange-correlation functional was used together with the vdW-TS[55] dispersion correction.

To obtain the properties of the individual molecules, we performed calculations with open boundary conditions. The geometry of the (charge-neutral) molecules was fully relaxed until the remaining forces on each atom fell below 0.01 eV/Å. From the optimized geometry, we extracted the orbital energies of the HOMO and LUMO, the molecular dipole moment, and the polarizability (via density functional perturbation theory[56]). Furthermore, we calculated the vertical

https://doi.org/10.1021/acsomega.1c05092
ACS Omega 2021, 6, 32270−32276

IP and EA using the so-called ΔSCF-approach.[57,58] There, these energies are given as the energy difference between the singly charged and the uncharged molecule while keeping the geometry of the neutral molecule. The singly charged molecules are calculated spin-polarized (which is not necessary for the neutral molecules). We employed a Gaussian occupation scheme with a broadening of 0.01 eV.

All other calculations (free-standing monolayer, metal−organic interfaces, and bare metals) were performed with periodic boundary conditions. Calculations for the bare substrate as well as for metal−organic interfaces were performed using five metal layers. We employed a repeated slab approach to emulate two-dimensional periodicity. The unit cell heights were chosen so that the vacuum amounts to at least 50 Å. To electrostatically decouple the periodic replica in the *z*-direction, we used a dipole correction.[28] The SCF algorithm was repeated until total energies in subsequent iterations differed by less than 10^{-5} eV and electron densities differed by less than 10^{-3} electrons. Furthermore, we ensured for all calculations that the change in the work function is converged to better than 10^{-4} eV between subsequent SCF iterations, as suggested by best practices.[54] We employed a generalized Monkhorst−Pack k-point grid[59,60] that corresponds to 50 × 50 × 1 k-points for the primitive substrate cells. Furthermore, a Gaussian occupation scheme with a broadening of 0.1 eV was used.

■ ASSOCIATED CONTENT

Supporting Information

The Supporting Information is available free of charge at https://pubs.acs.org/doi/10.1021/acsomega.1c05092.

Visualization of systems in the data set, comparison of our method and SISSO, finding concurrent effects, listing of naphthalene-derived adsorbates, calculation of image plane positions, data set sanity checks and analysis of alternative input parameters, and nonlinear mappings for expression generation (PDF)

■ AUTHOR INFORMATION

Corresponding Author

Oliver T. Hofmann − *Institute of Solid State Physics, Graz University of Technology, 8010 Graz, Austria;* orcid.org/0000-0002-2120-3259; Email: o.hofmann@tugraz.at

Authors

Johannes J. Cartus − *Institute of Solid State Physics, Graz University of Technology, 8010 Graz, Austria;* orcid.org/0000-0002-6353-2069

Andreas Jeindl − *Institute of Solid State Physics, Graz University of Technology, 8010 Graz, Austria;* orcid.org/0000-0002-2436-0073

Complete contact information is available at: https://pubs.acs.org/10.1021/acsomega.1c05092

Notes

The authors declare no competing financial interest.

All DFT calculations are available in the NOMAD repository (dx.doi.org/10.17172/NOMAD/2021.10.27-1).

■ ACKNOWLEDGMENTS

The authors thank Lukas Hörmann for his support and helpful insights. Funding through the project of the Austrian Science Fund (FWF): Y1157-N36 "MAP-DESIGN" is gratefully acknowledged. Computational results have been achieved using the Vienna Scientific Cluster (VSC).

■ REFERENCES

(1) Otero, R.; Vázquez de Parga, A. L.; Gallego, J. M. Electronic, Structural and Chemical Effects of Charge-Transfer at Organic/Inorganic Interfaces. *Surf. Sci. Rep.* **2017**, *72*, 105−145.

(2) Ishii, H.; Sugiyama, K.; Ito, E.; Seki, K. Energy Level Alignment and Interfacial Electronic Structures at Organic/Metal and Organic/Organic Interfaces. *Adv. Mater.* **1999**, *11*, 605−625.

(3) Zojer, E.; Taucher, T. C.; Hofmann, O. T. The Impact of Dipolar Layers on the Electronic Properties of Organic/Inorganic Hybrid Interfaces. *Adv. Mater. Interfaces* **2019**, *6*, No. 1900581.

(4) Braun, S.; Salaneck, W. R.; Fahlman, M. Energy-Level Alignment at Organic/Metal and Organic/Organic Interfaces. *Adv. Mater.* **2009**, *21*, 1450−1472.

(5) Koch, N. Organic Electronic Devices and Their Functional Interfaces. *ChemPhysChem* **2007**, *8*, 1438−1455.

(6) Sekitani, T.; Yokota, T.; Zschieschang, U.; Klauk, H.; Bauer, S.; Takeuchi, K.; Takamiya, M.; Sakurai, T.; Someya, T. Organic Nonvolatile Memory Transistors for Flexible Sensor Arrays. *Science* **2009**, *326*, 1516−1519.

(7) Klauk, H. Organic Thin-Film Transistors. *Chem. Soc. Rev.* **2010**, *39*, 2643−2666.

(8) Oehzelt, M.; Koch, N.; Heimel, G. Organic Semiconductor Density of States Controls the Energy Level Alignment at Electrode Interfaces. *Nat. Commun.* **2014**, *5*, 4174.

(9) Hörmann, L.; Jeindl, A.; Egger, A. T.; Scherbela, M.; Hofmann, O. T. SAMPLE: Surface Structure Search Enabled by Coarse Graining and Statistical Learning. *Comput. Phys. Commun.* **2019**, *244*, 143−155.

(10) Vazquez, H. Barrier Formation at Metal/Organic Interfaces: Dipole Formation and the Charge Neutrality Level. *Appl. Surf. Sci.* **2004**, *234*, 107−112.

(11) Vázquez, H.; Oszwaldowski, R.; Pou, P.; Ortega, J.; Pérez, R.; Flores, F.; Kahn, A. Dipole Formation at Metal/PTCDA Interfaces: Role of the Charge Neutrality Level. *Europhys. Lett.* **2004**, *65*, 802−808.

(12) Vazquez, H.; Flores, F.; Kahn, A. Induced Density of States Model for Weakly-Interacting Organic Semiconductor Interfaces. *Org. Electron.* **2007**, *8*, 241−248.

(13) Flores, F.; Ortega, J.; Vázquez, H. Modelling Energy Level Alignment at Organic Interfaces and Density Functional Theory. *Phys. Chem. Chem. Phys.* **2009**, *11*, 8658−8675.

(14) Braun, S.; Osikowicz, W.; Wang, Y.; Salaneck, W. R. Energy Level Alignment Regimes at Hybrid Organic-Organic and Inorganic-Organic Interfaces. *Org. Electron.* **2007**, *8*, 14−20.

(15) Braun, S.; Salaneck, W. R. Fermi Level Pinning at Interfaces with Tetrafluorotetracyanoquinodimethane (F4-TCNQ): The Role of Integer Charge Transfer States. *Chem. Phys. Lett.* **2007**, *438*, 259−262.

(16) Lindell, L.; Unge, M.; Osikowicz, W.; Stafström, S.; Salaneck, W. R.; Crispin, X.; de Jong, M. P. Integer Charge Transfer at the Tetrakis(Dimethylamino)Ethylene/Au Interface. *Appl. Phys. Lett.* **2008**, *92*, 163302.

(17) Romaner, L.; Heimel, G.; Brédas, J.-L.; Gerlach, A.; Schreiber, F.; Johnson, R. L.; Zegenhagen, J.; Duhm, S.; Koch, N.; Zojer, E. Impact of Bidirectional Charge Transfer and Molecular Distortions on the Electronic Structure of a Metal-Organic Interface. *Phys. Rev. Lett.* **2007**, *99*, No. 256801.

(18) Hofmann, O. T.; Egger, D. A.; Zojer, E. Work-Function Modification beyond Pinning: When Do Molecular Dipoles Count? *Nano Lett.* **2010**, *10*, 4369−4374.

(19) Hofmann, O. T.; Atalla, V.; Moll, N.; Rinke, P.; Scheffler, M. Interface Dipoles of Organic Molecules on Ag(111) in Hybrid Density-Functional Theory. *New J. Phys.* **2013**, *15*, No. 123028.

(20) Heimel, G.; Duhm, S.; Salzmann, I.; Gerlach, A.; Strozecka, A.; Niederhausen, J.; Bürker, C.; Hosokai, T.; Fernandez-Torrente, I.; Schulze, G.; Winkler, S.; Wilke, A.; Schlesinger, R.; Frisch, J.; Bröker,

B.; Vollmer, A.; Detlefs, B.; Pflaum, J.; Kera, S.; Franke, K. J.; Ueno, N.; Pascual, J. I.; Schreiber, F.; Koch, N. Charged and Metallic Molecular Monolayers through Surface-Induced Aromatic Stabilization. *Nat. Chem.* **2013**, *5*, 187−194.
(21) Ma, Z.; Rissner, F.; Wang, L.; Heimel, G.; Li, Q.; Shuai, Z.; Zojer, E. Electronic Structure of Pyridine -Based SAMs on Flat Au(111) Surfaces: Extended Charge Rearrangements and Fermi Level Pinning. *Phys. Chem. Chem. Phys.* **2011**, *13*, 9747−9760.
(22) Schmidt, M.; Lipson, H. Distilling Free-Form Natural Laws from Experimental Data. *Science* **2009**, *324*, 81−85.
(23) Wang, Y.; Wagner, N.; Rondinelli, J. M. Symbolic Regression in Materials Science. *MRS Commun.* **2019**, *9*, 793−805.
(24) Ouyang, R.; Curtarolo, S.; Ahmetcik, E.; Scheffler, M.; Ghiringhelli, L. M. SISSO: A Compressed-Sensing Method for Identifying the Best Low-Dimensional Descriptor in an Immensity of Offered Candidates. *Phys. Rev. Mater.* **2018**, *2*, 1−11.
(25) Heimel, G.; Romaner, L.; Bredas, J. L.; Zojer, E. Organic/Metal Interfaces in Self-Assembled Monolayers of Conjugated Thiols: A First-Principles Benchmark Study. *Surf. Sci.* **2006**, *600*, 4548−4562.
(26) Blum, V.; Gehrke, R.; Hanke, F.; Havu, P.; Havu, V.; Ren, X.; Reuter, K.; Scheffler, M. Ab Initio Molecular Simulations with Numeric Atom-Centered Orbitals. *Comput. Phys. Commun.* **2009**, *180*, 2175−2196.
(27) Perdew, J. P.; Burke, K.; Ernzerhof, M. Generalized Gradient Approximation Made Simple. *Phys. Rev. Lett.* **1996**, *77*, 3865−3868.
(28) Neugebauer, J.; Scheffler, M. Adsorbate-Substrate and Adsorbate-Adsorbate Interactions of Na and K Adlayers on Al(111). *Phys. Rev. B* **1992**, *46*, 16067−16080.
(29) Topping, J. On the Mutual Potential Energy of a Plane Network of Doublets. *Proc. R. Soc. London, Ser. A* **1927**, *114*, 67−72.
(30) Maschhoff, B. L.; Cowin, J. P. Corrected Electrostatic Model for Dipoles Adsorbed on a Metal Surface. *J. Chem. Phys.* **1994**, *101*, 8138−8151.
(31) Monti, O. L. A. Understanding Interfacial Electronic Structure and Charge Transfer: An Electrostatic Perspective. *J. Phys. Chem. Lett.* **2012**, *3*, 2342−2351.
(32) Natan, A.; Zidon, Y.; Shapira, Y.; Kronik, L. Cooperative Effects and Dipole Formation at Semiconductor and Self-Assembled-Monolayer Interfaces. *Phys. Rev. B: Condens. Matter Mater. Phys.* **2006**, *73*, 1−4.
(33) Romaner, L.; Heimel, G.; Zojer, E. Electronic Structure of Thiol-Bonded Self-Assembled Monolayers: Impact of Coverage. *Phys. Rev. B* **2008**, *77*, No. 045113.
(34) Verwüster, E.; Hofmann, O. T.; Egger, D. A.; Zojer, E. Electronic Properties of Biphenylthiolates on Au(111): The Impact of Coverage Revisited. *J. Phys. Chem. C* **2015**, *119*, 7817−7825.
(35) Bauert, T.; Zoppi, L.; Koller, G.; Garcia, A.; Baldridge, K. K.; Ernst, K.-H. Large Induced Interface Dipole Moments without Charge Transfer: Buckybowls on Metal Surfaces. *J. Phys. Chem. Lett.* **2011**, *2*, 2805−2809.
(36) Bröker, B.; Hofmann, O. T.; Rangger, G. M.; Frank, P.; Blum, R.-P.; Rieger, R.; Venema, L.; Vollmer, A.; Müllen, K.; Rabe, J. P.; Winkler, A.; Rudolf, P.; Zojer, E.; Koch, N. Density-Dependent Reorientation and Rehybridization of Chemisorbed Conjugated Molecules for Controlling Interface Electronic Structure. *Phys. Rev. Lett.* **2010**, *104*, No. 246805.
(37) Hofmann, O. T.; Glowatzki, H.; Bürker, C.; Rangger, G. M.; Bröker, B.; Niederhausen, J.; Hosokai, T.; Salzmann, I.; Blum, R.-P.; Rieger, R.; Vollmer, A.; Rajput, P.; Gerlach, A.; Müllen, K.; Schreiber, F.; Zojer, E.; Koch, N.; Duhm, S. Orientation-Dependent Work-Function Modification Using Substituted Pyrene-Based Acceptors. *J. Phys. Chem. C* **2017**, *121*, 24657−24668.
(38) Egger, A. T.; Hörmann, L.; Jeindl, A.; Scherbela, M.; Obersteiner, V.; Todorović, M.; Rinke, P.; Hofmann, O. T. Charge Transfer into Organic Thin Films: A Deeper Insight through Machine-Learning-Assisted Structure Search. *Adv. Sci.* **2020**, No. 2000992.
(39) Duhm, S.; Heimel, G.; Salzmann, I.; Glowatzki, H.; Johnson, R. L.; Vollmer, A.; Rabe, J. P.; Koch, N. Orientation-Dependent Ionization Energies and Interface Dipoles in Ordered Molecular Assemblies. *Nat. Mater.* **2008**, *7*, 326−332.
(40) Topham, B. J.; Kumar, M.; Soos, Z. G. Profiles of Work Function Shifts and Collective Charge Transfer in Submonolayer Metal-Organic Films. *Adv. Funct. Mater.* **2011**, *21*, 1931−1940.
(41) Hofmann, O. T.; Deinert, J.-C.; Xu, Y.; Rinke, P.; Stähler, J.; Wolf, M.; Scheffler, M. Large Work Function Reduction by Adsorption of a Molecule with a Negative Electron Affinity: Pyridine on ZnO($10\bar{1}0$). *J. Chem. Phys.* **2013**, *139*, 174701.
(42) Goronzy, D. P.; Ebrahimi, M.; Rosei, F.; Arramel; Fang, Y.; De Feyter, S.; Tait, S. L.; Wang, C.; Beton, P. H.; Wee, A. T. S.; Weiss, P. S.; Perepichka, D. F. Supramolecular Assemblies on Surfaces: Nanopatterning, Functionality, and Reactivity. *ACS Nano* **2018**, *12*, 7445−7481.
(43) Blowey, P. J.; Haags, A.; Rochford, L. A.; Felter, J.; Warr, D. A.; Duncan, D. A.; Lee, T.-L.; Costantini, G.; Kumpf, C.; Woodruff, D. P. Characterization of Growth and Structure of TCNQ Phases on Ag(111). *Phys. Rev. Mater.* **2019**, *3*, No. 116001.
(44) Franco-Canellas, A.; Duhm, S.; Gerlach, A.; Schreiber, F. Binding and Electronic Level Alignment of π-Conjugated Systems on Metals. *Rep. Prog. Phys.* **2020**, *83*, No. 066501.
(45) Offenbacher, H.; Lüftner, D.; Ules, T.; Reinisch, E. M.; Koller, G.; Puschnig, P.; Ramsey, M. G. Orbital Tomography: Molecular Band Maps, Momentum Maps and the Imaging of Real Space Orbitals of Adsorbed Molecules. *J. Electron Spectrosc. Relat. Phenom.* **2015**, *204*, 92−101.
(46) Schuler, B.; Liu, W.; Tkatchenko, A.; Moll, N.; Meyer, G.; Mistry, A.; Fox, D.; Gross, L. Adsorption Geometry Determination of Single Molecules by Atomic Force Microscopy. *Phys. Rev. Lett.* **2013**, *111*, No. 106103.
(47) Lackinger, M.; Griessl, S.; Heckl, W. M.; Hietschold, M. Coronene on Ag(111) Investigated by LEED and STM in UHV. *J. Phys. Chem. B* **2002**, *106*, 4482−4485.
(48) Pearson, R. G. Acids and Bases. *Science* **1966**, *151*, 172−177.
(49) Körzdörfer, T.; Kümmel, S.; Marom, N.; Kronik, L. When to Trust Photoelectron Spectra from Kohn-Sham Eigenvalues: The Case of Organic Semiconductors. *Phys. Rev. B* **2009**, *79*, No. 201205 R.
(50) Wruss, E.; Zojer, E.; Hofmann, O. T. Distinguishing between Charge-Transfer Mechanisms at Organic/Inorganic Interfaces Employing Hybrid Functionals. *J. Phys. Chem. C* **2018**, *122*, 14640−14653.
(51) Ruiz, V. G.; Liu, W.; Zojer, E.; Scheffler, M.; Tkatchenko, A. Density-Functional Theory with Screened van Der Waals Interactions for the Modeling of Hybrid Inorganic-Organic Systems. *Phys. Rev. Lett.* **2012**, *108*, No. 146103.
(52) Ruiz, V. G.; Liu, W.; Tkatchenko, A. Density-Functional Theory with Screened van Der Waals Interactions Applied to Atomic and Molecular Adsorbates on Close-Packed and Non-Close-Packed Surfaces. *Phys. Rev. B* **2016**, *93*, 1−17.
(53) Hörmann, L.; Jeindl, A.; Hofmann, O. T. Reproducibility of Potential Energy Surfaces of Organic/Metal Interfaces on the Example of PTCDA on Ag(111). *J. Chem. Phys.* **2020**, *153*, 104701.
(54) Hofmann, O. T.; Zojer, E.; Hörmann, L.; Jeindl, A.; Maurer, R. J. First-Principles Calculations of Hybrid Inorganic-Organic Interfaces: From State-of-the-Art to Best Practice. *Phys. Chem. Chem. Phys.* **2021**, *23*, 8132−8180.
(55) Tkatchenko, A.; Scheffler, M. Accurate Molecular Van Der Waals Interactions from Ground-State Electron Density and Free-Atom Reference Data. *Phys. Rev. Lett.* **2009**, *102*, No. 073005.
(56) Shang, H.; Raimbault, N.; Rinke, P.; Scheffler, M.; Rossi, M.; Carbogno, C. All-Electron, Real-Space Perturbation Theory for Homogeneous Electric Fields: Theory, Implementation, and Application within DFT. *New J. Phys.* **2018**, *20*, 073040.
(57) Hellman, A.; Razaznejad, B.; Lundqvist, B. I. Potential-Energy Surfaces for Excited States in Extended Systems. *J. Chem. Phys.* **2004**, *120*, 4593−4602.
(58) Noe, M.; Heller, R.; Fietz, W. H.; Goldacker, W.; Schneider, T. *HTS Applications. Proc.—Workshop Accelerator magnet superconductors, design and optimization, WAMSDO 2008;* 2009; pp 94−97.

https://doi.org/10.1021/acsomega.1c05092
ACS Omega 2021, 6, 32270−32276

(59) Monkhorst, H. J.; Pack, J. D. Special Points for Brillouin-Zone Integrations. *Phys. Rev. B* **1976**, *13*, 5188−5192.
(60) Wisesa, P.; McGill, K. A.; Mueller, T. Efficient Generation of Generalized Monkhorst-Pack Grids through the Use of Informatics. *Phys. Rev. B* **2016**, *93*, No. 155109.

NOTE ADDED AFTER ASAP PUBLICATION

This paper was published on November 14, 2021, with incorrect versions of the Supporting Information file and Abstract graphic, and an incorrect title for Table 2. The corrected version was reposted on November 16, 2021.

https://doi.org/10.1021/acsomega.1c05092
ACS Omega 2021, 6, 32270−32276